Naunyn-Schmiedeberg's Archives of Pharmacology
https://doi.org/10.1007/s00210-019-01753-9

ORIGINAL ARTICLE

Synthesis, pharmacological evaluation and molecular docking of novel *R*-/*S*-2-(2-hydroxypropanamido)-5-trifluoromethyl benzoic acid as dual anti-inflammatory anti-platelet aggregation agents

Rong Rong[1] · Rui-zhen Zhang[1] · Xin Wang[1] · Yu-han Dan[1] · Yun-li Zhao[1] · Zhi-guo Yu[1]

Received: 10 May 2019 / Accepted: 18 October 2019

Abstract

R-/*S*-2-(2-hydroxypropanamido) benzoic acid (*R*-/*S*-HPABA), marine-derived anti-inflammatory antiplatelet drugs, were initially synthesised in our group. However, preliminary research showed that *R*-/*S*-HPABA were eliminated rapidly because of extensive hydroxylation metabolism of phenyl ring in vivo. In order to reduce significant hydroxylation metabolism to improve pharmacological activity and bioavailability, trifluoromethyl group was incorporated into *R*-/*S*-HPABA to synthesise *R*-/*S*-2-(2-hydroxypropanamido)-5-trifluoromethyl benzoic acid (*R*-/*S*-HFBA), respectively. The purposes of this study were to report the synthesis of *R*-/*S*-HFBA and compare the anti-inflammatory antiplatelet effect and pharmacokinetic properties of *R*-/*S*-HFBA with those of *R*-/*S*-HPABA. Carrageenan-induced rat paw edema assay was used for the evaluation of the anti-inflammatory activity. *R*-/*S*-HFBA showed better results in inhibiting edema and were able to prolong the anti-inflammatory effect after carrageenan injection. The antiplatelet aggregation activity of *R*-/*S*-HFBA and *R*-/*S*-HPABA was studied on arachidonic acid-induced platelet aggregation of rabbit platelet-rich plasma. The aggregation inhibition rate of *R*-/*S*-HFBA was significantly ($p < 0.05$) higher than that of *R*-/*S*-HPABA, respectively. Molecular docking study revealed that *R*-/*S*-HFBA possess more potent binding affinity with COX-1/COX-2 than *R*-/*S*-HPABA, respectively, and that the presence of trifluoromethyl group leads to increase in activity of *R*-/*S*-HFBA. *R*-/*S*-HFBA also afford more favorable pharmacokinetic properties than *R*-/*S*-HPABA, respectively, such as higher C_{max}, larger $AUC_{0\text{-}\infty}$, and longer $t_{1/2}$, which, as expected, are more metabolically stable.

Keywords *R*-/*S*-2-(2-hydroxypropanamido) benzoic acid · *R*-/*S*-2-(2-hydroxypropanamido)-5-trifluoromethyl benzoic acid · Anti-inflammatory · Antiplatelet · Molecular docking

Introduction

Inflammation, one of the most crucial protective mechanisms of the body against irritation, tissue lesion or infection, is able to induce cellular damage and release pro-inflammatory mediators (Newton and Dixit 2012; Maurent et al. 2017). Non-steroidal anti-inflammatory drugs (NSAIDs) are the most common therapeutic agents through their anti-inflammatory, analgesic antipyretic effect (Fiorucci et al. 2001; Rao et al. 2010). The anti-inflammatory activity of NSAIDs is due to the inhibition of cyclooxygenase (COX) involved in the production of pro-inflammatory prostaglandins (PGs) and thromboxanes (TXs). COX has two main isoforms: COX-1 is the naturally expressed isozyme that is related with homeostatic prostanoid biosynthesis under physiological conditions. In particular, aspirin also can inhibit COX-1 in the platelets, suppress arachidonic acid (AA) metabolism, and prevent the synthesis of thromboxane A_2 (TXA_2), a compound that induces platelet aggregation. COX-2 is inducibly expressed by inflammatory stimulant from infections or injuries (Woo and Kwon 2007; Helmersson et al. 2005; Vane and Botting 1987; Catella-Lawson et al. 2001). However, long-term clinical use of NSAIDs, particularly aspirin, may lead to significant side effects, mainly gastrointestinal, cardiovascular and renal (Lazzaroni and Bianchi 2004; Ashour et al. 2013). Thus, there is an unmet medical need for developing more effective and safe anti-inflammatory drugs to supplement or replace the current therapies.

✉ Yun-li Zhao
yunli76@163.com

✉ Zhi-guo Yu
zhiguo-yu@163.com

[1] Department of Pharmaceutical Analysis, School of Pharmacy, Shenyang Pharmaceutical University, Shenyang 110016, China

Published online: 05 December 2019

Fluorine continues to make great contribution to the design and development of biologically active compounds. About 20% of the currently used drugs and agrochemicals are fluorine-containing organic molecules (Wang et al. 2014; Purser et al. 2008; Gouverneur and Müller 2012). It is well known that incorporation of fluorine or various fluorinated substituents into an organic molecule has had a tremendous impact on physical and chemical properties such as solubility, lipophilicity or biological potency (Cho et al. 2010; Sorochinsky and Soloshonok 2010; Acena et al. 2013; Gillis et al. 2015). In several times, the drug-receptor interactions are also improved in the presence of fluorine moiety (Abid et al. 2012). Among multifarious fluorine substituents, trifluoromethyl group is one of the most important structural fragments, because its introduction into small molecules can enhance the effect of their interactions with cellular targets, improve cellular membrane permeability and increase stability by reducing oxidative metabolism (Liu et al. 2015; Ojima 2013; Mueller et al. 2007; Hagmann 2008). The trifluoromethyl fragment is a part of many biologically active molecules such as highly active antiretroviral therapy agent Sustiva, antidepressant Prozac, nonsteroidal anti-inflammatory agent Celebrex, antimalarial agent mefloquine and oral multikinase inhibitor sorafenib (Liu et al. 2015; Dey et al. 2018; Russo et al. 2016; Palmer et al. 1993; Hasskarl 2014). Incorporating a trifluoromethyl group into biologically important compounds or into already known pharmaceutical agents has been widely accepted as a powerful tool to enhance the activity of these agents (Ismail 2002; Tressaud and Haufe 2008; Kulikova et al. 2017).

S-2-(2-hydroxypropanamido) benzoic acid (*S*-HPABA; Fig. 1), which was initially isolated from the fermentation broth of a marine fungus Penicillium chrysogenum by our group, presented anti-inflammatory activity like aspirin, but no gastrointestinal toxicity (Wang et al. 2014a; Yu et al. n.d.). To research further on *S*-HPABA, a simple and efficient stereospecific synthetic route was developed for *S*-HPABA, as well as *R*-2-(2-hydroxypropanamido) benzoic acid (*R*-HPABA; Fig. 1), the *R*-enantiomer (Wang et al. 2014b). Moreover, our previous study showed that *R*-/*S*-HPABA also exhibited remarkable antiplatelet aggregation and antithrombosis effect like aspirin (Zhang et al. 2017). But preliminary researches indicated that *S*-HPABA was eliminated rapidly because of widely phase I and phase II metabolic reactions in vivo. Hydroxylation metabolite of phenyl ring was the main metabolite of *S*-HPABA in rats (Guan et al. 2015).

In order to reduce significant hydroxylation metabolism to improve pharmacological activity and bioavailability, trifluoromethyl group was incorporated into *R*-/*S*-HPABA to synthesise *R*-/*S*-2-(2-hydroxypropanamido)-5-trifluoromethyl benzoic acid (*R*-/*S*-HFBA; Fig. 1) in our laboratory for the first time. Herein, we report the synthesis of *R*-/*S*-HFBA and compare the pharmacodynamics and pharmacokinetics properties

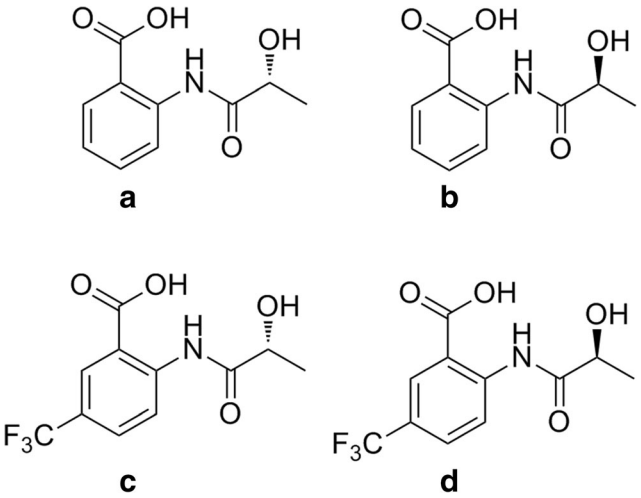

Fig. 1 Chemical structures of *R*-HPABA (**a**), *S*-HPABA (**b**), *R*-HFBA (**c**) and *S*-HFBA (**d**)

of *R*-/*S*-HFBA with those of *R*-/*S*-HPABA. The structure activity relationship was also discussed, and the results have been confirmed by molecular docking calculations. Results of this investigation provide valuable scientific research data and probably play an important role in the discovery of novel anti-inflammatory antiplatelet aggregation drug.

Material and methods

Materials

R-/*S*-HPABA and *R*-/*S*-HFBA (optical purity of all compounds > 99.0%) were, respectively, synthesised in our laboratory. Aspirin (purity > 99.5%) was purchased from Shanghai Aladdin biochemical technology Co., Ltd (Shanghai, China). For in vitro study, *R*-/*S*-HPABA and *R*-/*S*-HFBA were dissolved and diluted by dimethyl sulfoxide (DMSO). In vivo studies, *R*-/*S*-HPABA and *R*-/*S*-HFBA were suspended in 0.5% aqueous solution of sodium carboxymethyl cellulose for oral administration and dissolved in normal saline for intravenous administration.

Chemistry

The chemical reagents and solvents used were purchased from commercial vendors and used without purification. Melting points were determined on a Buchi apparatus and were uncorrected. IR spectra were recorded on a Bruker IFS-55 spectrometer. NMR spectra were determined on Brucker 600 M AVIII spectrophotometer. The chemical shifts were given in δ units and coupling constants (*J*) were measured in Hertz (Hz). Signals are described as s (singlet), d (doublet), t (triplet), q (quartet), m (multiplet), dd (double doublet). Mass spectra were recorded on Agilent 6540 UHD Q-TOF mass

spectrometer. TLC development was conducted on silica gel sheets. The spots were visualised by exposure to UV-lamp at λ 254 nm.

Synthesis

Synthesis of the intermediate and target compound is illustrated in Scheme 1. In the synthetic approach, *S*-HFBA was prepared using *L*-lactic acid as starting material while *R*-HFBA was obtained starting with *D*-lactic acid in a total yield of 60.2%. Compounds 2 and 3 were synthesised according to previously published literature procedures (Wang et al. 2014b).

Synthesis of *S*-methyl 2-(2-acetoxypropionyl amino) -5-trifluoromethyl benzoate compound 4

To a stirred suspension of *S*-methyl 2-amino-5-trifluoromethyl benzoate (4.2 g, 19.2 mmol) in diethyl ether (300 mL), compound 3 (11.56 g, 76.8 mmol) was added dropwise at − 10–0 °C. The reaction mixture was stirred at room temperature for 3 h. After the completion of reaction (monitored by TLC), mixture was washed with hydrochloric acid, water, $NaHCO_3$ solution, and aqueous saturated sodium chloride then dried over Na_2SO_4. The dried extract was filtered and concentrated under reduced pressure to give *S*-methyl 2-(2-acetoxypropionyl amino)-5-trifluoromethyl benzoate compound 4 (5.87 g, 92.0%).

General procedure for synthesis of *S*-2-(2-hydroxypropanamido)-5-trifluoromethyl benzoic acid

To a solution of compound 4 (5.87 g, 17.6 mmol) in 40 mL methanol and 60 mL tetrahydrofuran, 10% sodium hydroxide was added and stirred at room temperature for 3–4 h. After then, the reaction mixture was extracted with CH_2Cl_2 three times. The aqueous layer was acidised to pH = 1–4 by addition of HCl until crystal appeared. It was then kept in freezer overnight. The product obtained was filtered, collected and dried at 40 °C to give *S*-2-(2-hydroxypropanamido)-5-trifluoromethyl benzoic acid. The expected compound was obtained as white crystalline powder, pure enough to be used without further purification. Yield 4.57 g, 93.7%; m.p. 146–148 °C; $[\alpha]_D^{20}$: − 12.2° (c = 0.5 g/100 mL, MeOH); IR (KBr, cm^{-1}): 3388, 3206, 1690, 1668; ^{1}H NMR (MeOH-d_4, 600 MHz): δ 1.45 (d, 3H, CH_3), 3.35 (s, 1H, CH-OH), 4.28 (q, 1H, CH-OH), 7.85 (d, 1H, Ar-H), 8.34 (brs, 1H, Ar-H), 8.93 (d, 1H, Ar-H); ^{13}C NMR (MeOH-d_4, 150 MHz): δ 21.0 (s, CH_3), 69.9 (s, CH-OH), 177.2 (s, -CO-NH), 169.4 (s, COOH), 125.2 (q, J = 270 Hz, CF_3), 118.1(s, C-1), 144.9 (s, C-2), 121.5 (s, C-3), 131.6 (q, J = 3 Hz, C-4), 125.6 (q, J = 30 Hz, C-5), 129.6 (q, J = 3 Hz, C-6); ^{19}F NMR (MeOH-d_4): − 63.96 (s, 3F, CF_3); HRMS m/z calcd for $C_{11}H_{10}NF_3O_4$ $[M-H]^-$: 276.0489, found: 276.0520.

Pharmacology

Experimental animals

Male Sprague-Dawley rats at age 7–8 weeks and New Zealand white male rabbits at age 3 months were provided by Experimental Animal Center, Shenyang Pharmaceutical University (Shenyang, China). Animals were kept in plastic cages in standard environmental conditions and had free access to standard diet with water ad libitum. The animals were fasted for 12 h with only access to water prior to experimentation. All experimental studies were performed in accordance with the Guideline for Animal Experimentation of Shenyang Pharmaceutical University and the approval from Animal Ethics Committee of Shenyang Pharmaceutical University.

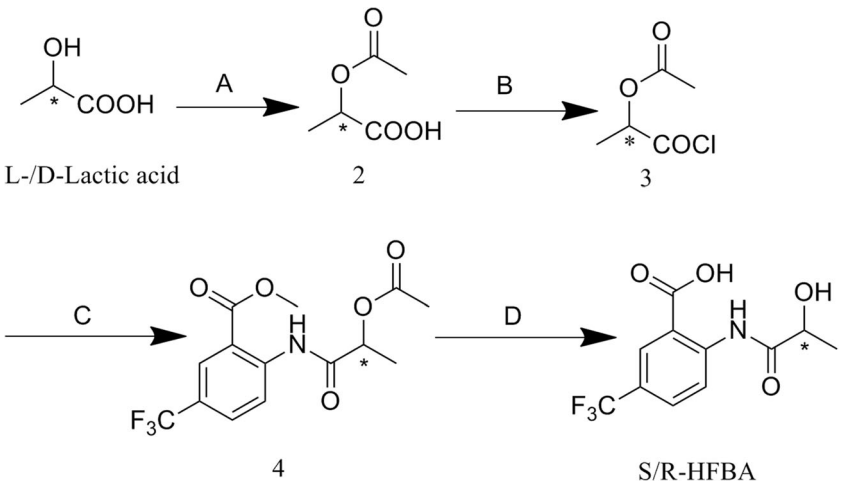

Scheme 1 Synthesis of *R*-/*S*-HFBA. Reagents and conditions: **a** acetyl chloride, THF, 40 °C; **b** $SOCl_2$, 50 °C; **c** methyl 2-amino-5-trifluoromethyl benzoate; diethyl ether, room temperature; **d** MeOH, THF, NaOH, room temperature

Anti-inflammatory activity

Carrageenan-induced hind paw edema in rats was used for the evaluation of anti- inflammatory activity (Winter et al. 1962). Sprague-Dawley rats were randomly divided into ten groups (five rats in each group) and administered orally in the following manner. Initially, the first group was treated with 0.5% aqueous solution of sodium carboxymethyl cellulose (*w*/*v*) acting as a negative control. The second group was given aspirin as a reference standard (100 mg/kg). Rats in group 3 received 100 mg/kg of *S*-HPABA while rats in groups 4, 5, 6 received 50, 100, 200 mg/kg of *S*-HFBA, respectively. Rats in group 7 were given 100 mg/kg of *R*-HPABA while rats in groups 8, 9, 10 received 50, 100, 200 mg/kg of *R*-HFBA, respectively. The right hind paw edema was produced by sub-plantar injection of 0.1 mL of freshly prepared carrageenan (1%) in normal saline 1 h after the administration. The paw thickness was measured using vernier calipers and the difference between paw thickness was recorded at hourly intervals up to 5 h. The percentage edema (E%) and inhibition rate (I%) of each group were calculated as follows (Sayed et al. 2018):

$$\text{Edema rate (E\%)} = {}^{(PT_t - PT_0)}\Big/_{PT_0} \times 100\%$$

$$\text{Inhibition rate (I\%)} = {}^{(E_c - E_c)}\Big/_{E_c} \times 100\%$$

where PT_0 and PT_t are the paw thickness (mm) before and after carrageenan injection, respectively, and E_c and E_t are the average percentage edema of negative control group and the treated, respectively.

Determination of TNF-α and IL-1β levels in the rat paw

Five hours after carrageenan injection, inflamed hind paws were removed and stored at − 80 °C to be processed for TNF-α and IL-1β determinations. The paw tissue samples were weighed and homogenised in phosphate-buffered saline (pH = 7.4). The homogenates were centrifuged at 12,000×*g* for 20 min at 4 °C, and the supernatant was obtained to be kept at − 80 °C for cytokine assay. The TNF-α and IL-1β levels were determined by enzyme-linked immunosorbent assay (ELISA) kits (ABclonal Biotechnology Co., Ltd, USA) according to manufacturer's instructions.

Anti-platelet aggregation assay

The antiplatelet aggregation effect of *R*-/*S*-HFBA and *R*-/*S*-HPABA was studied on AA-induced platelet aggregation of rabbit platelet-rich plasma (PRP) (Zhang et al. 2017). Blood was collected from the carotid artery of rabbits and PRP was prepared by centrifugation of citrated blood at 1000 rpm for 15 min at room temperature. PRP samples (335 μL) with *R*-/*S*-HPABA or *R*-/*S*-HFBA at a concentration of 0.64 mol/mL (3.5 μL) were added into aggregometer cuvettes and aggregation was recorded as increased light transmission at 37 °C after the addition of the stimulus. AA at concentration of 20 μmol/mL (10 μL) was used as the platelet activator in PRP. PRP samples were pre-incubated at 37 °C for 2 min before the addition of AA. In blank and positive control experiments, DMSO (3.5 μL) and aspirin (3.5 μL) were added instead of the test samples, respectively. The percent inhibition rate was evaluated and calculated according to our previous report (Zhang et al. 2017).

Molecular docking

Docking study was performed to evaluate the binding mode and compare the binding affinity of *R*-/*S*-HFBA and *R*-/*S*-HPABA with COX-1/COX-2. With this purpose, crystal structures of COX-1 (PDB codes: 3N8Y) and COX-2 (PDB codes: 5IKT) were obtained from the PDB database (Sidhu et al. 2010; Orlando and Malkowski 2016). For protein preparation, water molecules, the repeating chains and other ligands were eliminated. Hydrogen atoms were added to the receptor and Gasteiger charges were calculated. The Lamarckian genetic algorithm (LGA) was applied to generate the best conformation of the compounds binding in COX-1/COX-2. The compounds were docked into the pocket of each protein center around binding site, with the LGA. After docking, the obtained poses with the lowest binding energy were selected as the most probable binding conformation. Discovery Studio 4.5 was chosen to show the docking results.

Pharmacokinetic study

R-/*S*-HFBA and *R*-HPABA were administered intravenously (12.5 mg/kg) and intragastricly (50 mg/kg) to conscious SD rats, respectively. Blood samples (approximately 0.25 mL) were drawn from fosse orbital vein at 0.033, 0.083, 0.25, 0.5, 0.75, 1, 1.5, 2, 2.5, 3, 4, 6 and 8 h after intravenous administration and at 0.083, 0.25, 0.5, 0.75, 1, 1.5, 2, 3, 4, 6, 8, 12 and 24 h after oral administration. The plasma concentration of drug was determined by HPLC method with liquid-liquid extraction. Pharmacokinetic parameters were calculated using non-compartmental analysis of DAS 2.1 pharmacokinetic program (Chinese Pharmacological Society).

Statistical analysis

Experimental results are expressed as mean ± standard deviation (SD). Statistical analysis was performed using Tukey's

Table 1 Effects of *R*-/*S*-HFBA and *R*-/*S*-HPABA on carrageenan-induced paw edema in rats (mean ± SD, $n = 5$)

Group	Dose (mg kg^{-1})	Edema rate (%) Inhibition rate (%)				
		1 h	2 h	3 h	4 h	5 h
Control	-	40.23 ± 3.07	79.74 ± 9.42	66.66 ± 8.88	60.59 ± 3.86	51.94 ± 4.26
ASP	100	25.84 ± 7.60**	53.37 ± 6.30**	45.58 ± 6.60**	41.98 ± 7.53***	39.84 ± 9.51*
		35.77	33.07	31.62	30.71	23.30
S-HPABA	100	22.70 ± 7.78**	41.25 ± 10.83***	40.98 ± 4.84***	39.60 ± 7.30***	36.01 ± 2.30***
		43.57	48.27	38.52	34.64	30.67
S-HFBA	50	29.97 ± 5.98**	54.37 ± 9.78**	47.29 ± 3.33**	43.48 ± 4.14***	42.13 ± 8.57
		25.50	31.82	29.06	28.24	18.89
	100	24.62 ± 6.39**	42.80 ± 8.73***	35.09 ± 6.63***	30.96 ± 5.64***	28.72 ± 6.36***
		38.80	46.33	47.36	48.90	44.71
	200	19.10 ± 5.25***	34.62 ± 8.06***	29.43 ± 8.19***	26.90 ± 8.61***	21.46 ± 7.47***
		52.52	56.58	55.85	55.60	58.56
R-HPABA	100	20.20 ± 5.70***	44.85 ± 9.64***	44.71 ± 11.12***	40.74 ± 6.98***	36.94 ± 9.61***
		49.79	43.75	32.93	32.76	28.88
R-HFBA	50	28.98 ± 5.97**	56.95 ± 5.48**	47.45 ± 2.28**	39.42 ± 7.10**	39.77 ± 7.21*
		27.96	28.58	28.82	34.94	23.43
	100	20.98 ± 1.47***	41.20 ± 7.64***	34.33 ± 6.25***	31.17 ± 6.26***	26.01 ± 8.05***
		47.85	48.33	48.50	48.56	49.92
	200	15.78 ± 5.62***	30.03 ± 7.11***	26.47 ± 3.55***	23.10 ± 4.73***	19.41 ± 3.91***
		60.78	62.34	60.29	61.87	62.63

$^{*}p < 0.05$, $^{**}p < 0.01$, $^{***}p < 0.001$ vs control group

test and one-way analysis of variance by SPSS Statistics 20.0. For a confidence interval of 95%, a value of $p < 0.05$ was indicative of significant.

Results

Anti-inflammatory activity

To evaluate the anti-inflammatory activity of *R*-/*S*-HFBA and *R*-/*S*-HPABA, the carrageenan-induced rat paw edema model was used (Winter et al. 1962; Sayed et al. 2018). The results of this assay are presented in Table 1. It showed that *R*-/*S*-HPABA (100 mg/kg) and all the doses tested for *R*-/*S*-HFBA considerably reduced paw edema after carrageenan administration ($p < 0.05$, $p < 0.01$, $p < 0.001$), compared to control group. *R*-/*S*-HFBA decreased the paw edema in a dose-dependent manner. Moreover, at the 100-mg/kg dose, the paw edema inhibition rates of *S*-HFBA were significantly higher (47.36%, 48.90%, 44.71%, respectively) than those of *S*-HPABA (38.52%, 34.64%, 30.67%, respectively) at 3, 4 and 5 h after the administration of carrageenan. After 2 h of administration, *R*-HFBA also showed a higher inhibition rate than *R*-HPABA at the same dose. The results suggested that the introduction of trifluoromethyl prolonged the anti-inflammatory effect of *R*-/*S*-HFBA.

Assay of TNF-α and IL-1β levels in carrageenan-injected paws

In order to observe the effects of *R*-/*S*-HFBA and *R*-/*S*-HPABA on inflammatory cytokine secretions, TNF-α and IL-1β levels in rat-inflamed paws were determined by enzyme-linked immunosorbent assay. As shown in Figs. 2 and 3, all of the tested compounds and the reference drug could significantly reduce the production of TNF-α and IL-1β, compared to the control group ($p < 0.05$, $p < 0.01$, $p < 0.001$). Moreover, *S*-HFBA signifcantly decreased the TNF-α and IL-1β levels compared to the *S*-HPABA group at the same dose ($p < 0.05$). The concentrations of TNF-α and IL-1β in *R*-HFBA group (100 mg/kg) were also significantly lower than that in *R*-HPABA group (100 mg/kg) ($p < 0.05$, $p < 0.01$), respectively.

Anti-platelet aggregation assay

Anti-aggregation effects of *R*-/*S*-HFBA and *R*-/*S*-HPABA were studied on AA-induced platelet aggregation. The results are presented in Fig. 4. It showed that *R*-/*S*-HFBA and *R*-/*S*-HPABA could significantly inhibit AA-induced platelet aggregation. There was a significant ($p < 0.05$) increase in the platelet aggregation inhibition by *S*-HFBA compared to *S*-HPABA. The aggregation inhibition rate was also

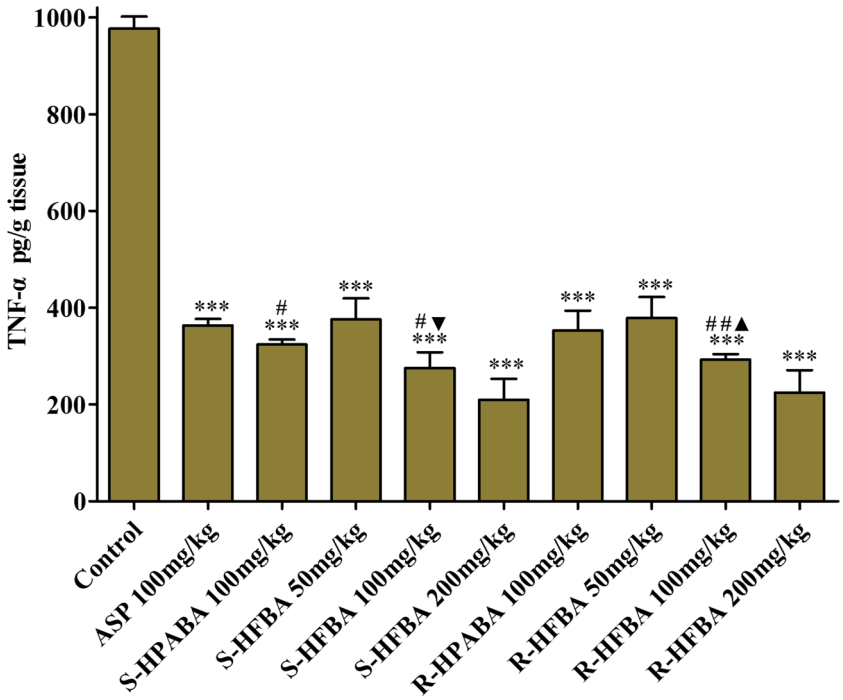

Fig. 2 Effect of *R*-/*S*-HPABA and *R*-/*S*-HFBA on TNF-α levels in the rat paws treated with carrageenan. The results are expressed as mean ± SD ($n = 5$). $^{*}p < 0.05$, $^{**}p < 0.01$, $^{*}p < 0.001$ vs control group $^{\#}p < 0.05$, $^{\#\#}p < 0.01$ vs ASP 100-mg/kg group; $^{\blacktriangledown}p < 0.05$, *S*-HFBA 100 mg/kg vs *S*-HPABA 100 mg/kg; $^{\blacktriangle}p < 0.05$, *R*-HFBA 100 mg/kg vs *R*-HPABA 100 mg/kg

significantly ($p < 0.05$) higher with *R*-HFBA than with *R*-HPABA. The results also clearly demonstrated that *R*-HFBA inhibited platelet aggregation more potently than the reference drug aspirin ($p < 0.01$).

Molecular docking

In order to compare the binding affinity of *R*-/*S*-HFBA and *R*-/*S*-HPABA with COX-1/COX-2, we docked all compounds to evaluate their molecular docking. Docking study had been performed from the selection of the X-ray structure. The X-ray structures of COX-1 and COX-2 were chosen from PDB database (PDB code 3N8Y and 5IKT). *S*-HPABA and *S*-HFBA bind to COX-1 enzyme by releasing free energy of − 7.67 and − 9.48 kcal/mol, respectively, and to COX-2 releasing free energy of − 7.14 and − 9.47 kcal/mol, respectively. The binding affinity of *R*-HPABA and *R*-HFBA to COX-1 showed score = − 7.85 and − 9.47

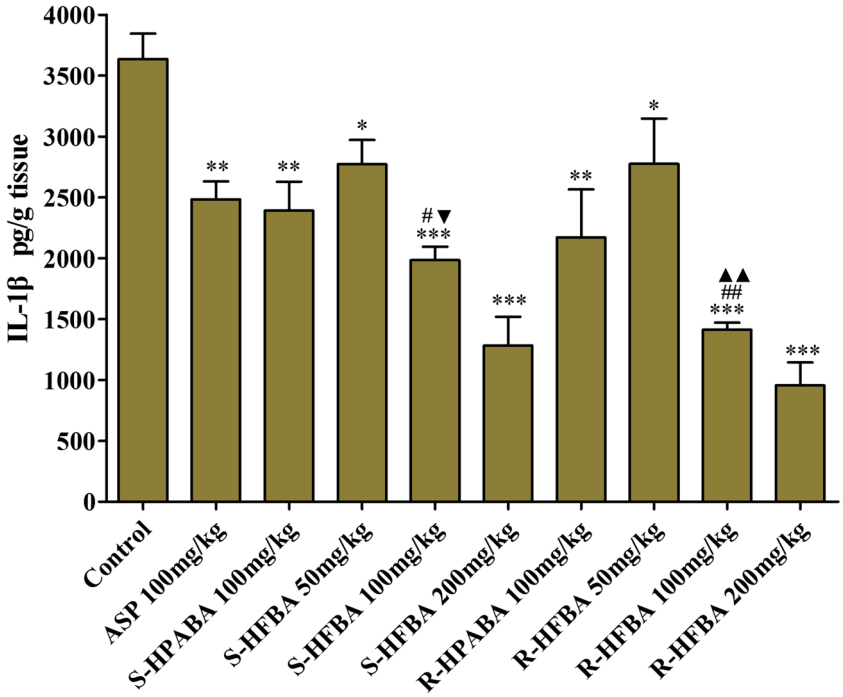

Fig. 3 Effect of *R*-/*S*-HPABA and *R*-/*S*-HFBA on IL-1β levels in the rat paws treated with carrageenan. The results are expressed as mean ± SD ($n = 5$). $^{*}p < 0.05$, $^{**}p < 0.01$, $^{*}p < 0.001$ vs control group; $^{\#}p < 0.05$, $^{\#\#}p < 0.01$ vs ASP 100-mg/kg group; $^{\blacktriangledown}p < 0.05$, *S*-HFBA 100 mg/kg vs *S*-HPABA 100 mg/kg; $^{\blacktriangle}p < 0.05$, $^{\blacktriangle\blacktriangle}p < 0.01$, *R*-HFBA 100 mg/kg vs *R*-HPABA 100 mg/kg

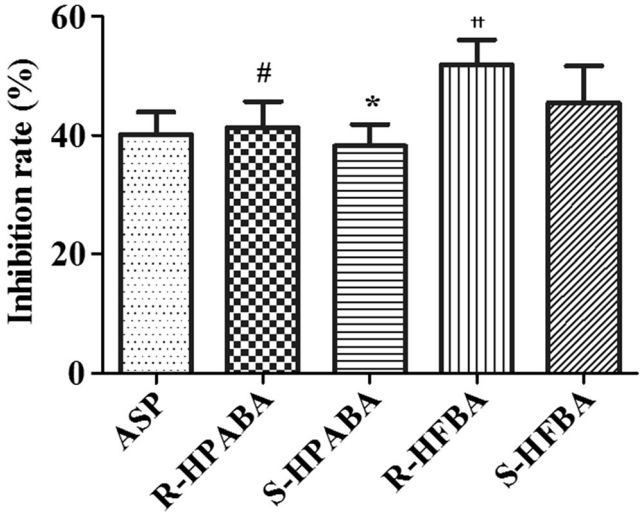

Fig. 4 The effects of *R*-/*S*-HPABA, *R*-/*S*-HFBA and aspirin (ASP) on the platelet aggregation induced by AA. Results are given as mean ± SD (n = 3). $^{\dagger}p < 0.05$, $^{\dagger\dagger}p < 0.01$ vs ASP; $^{*}p < 0.05$, $^{**}p < 0.01$ *S*-HPABA vs. *S*-HFBA; $^{\#}p < 0.05$, $^{\#\#}p < 0.01$ *R*-HPABA vs. *R*-HFBA

kcal/mol, respectively, and to COX-2 showed score = − 7.67 and − 9.54 kcal/mol, respectively. Binding mode of all compounds at COX-1/COX-2 active sites is presented in Figs. 5, 6, 7 and 8.

Pharmacokinetic study

Pharmacokinetic experiments were performed to compare the pharmacokinetic behavior and absolute bioavailability of *R*-/*S*-HPABA with those of *R*-/*S*-HFBA. Mean plasma concentration-time curves after intragastric and intravenous administration are shown in Figs. 9 and 10, respectively. The main pharmacokinetic parameters based on non-compartmental analysis are listed in Table 2 and Table 3. The results showed that the C_{max} and $AUC_{0\text{-}\infty}$ after the intragastric administration of *S*-HFBA were nearly 2.8-fold and 6.5-fold higher than that of *S*-HPABA, respectively. The C_{max} and $AUC_{0\text{-}\infty}$ after the intragastric administration of *R*-HFBA were nearly 3.7-fold and 13.1-fold higher than that of *R*-HPABA, respectively. Moreover, the elimination half-life ($t_{1/2}$) of *R*-/*S*-HFBA after the intragastric administration was significantly longer than that of *R*-/*S*-HPABA ($p < 0.01$, $p < 0.05$), respectively. Meanwhile, the clearance (CL) for *R*-/*S*-HFBA was found to be significantly lower than that of *R*-/*S*-HPABA ($p < 0.01$). The absolute bioavailability of *R*-/*S*-HFBA and *R*-/*S*-HPABA was 88.7%, 66.8%, 54.9% and 58.1%, respectively.

Discussion

R-HFBA had the same NMR, IR spectroscopy and MS data with *S*-HFBA while the $[\alpha]_D^{20}$ of *R*-HFBA was + 13.2°. The structure of *S*-HFBA was proven by IR spectral bands of –NHCO– at 1668 cm^{-1} and –NH stretching at 3206 cm^{-1}. Absorption peaks at 3388 cm^{-1} and 1690 cm^{-1}, due to carboxylic OH and C=O groups, respectively, were also observed. In the ^{1}H NMR spectra of compound, the hydrogens in the CH_3 group were found as a doublet peak at 1.45 ppm.

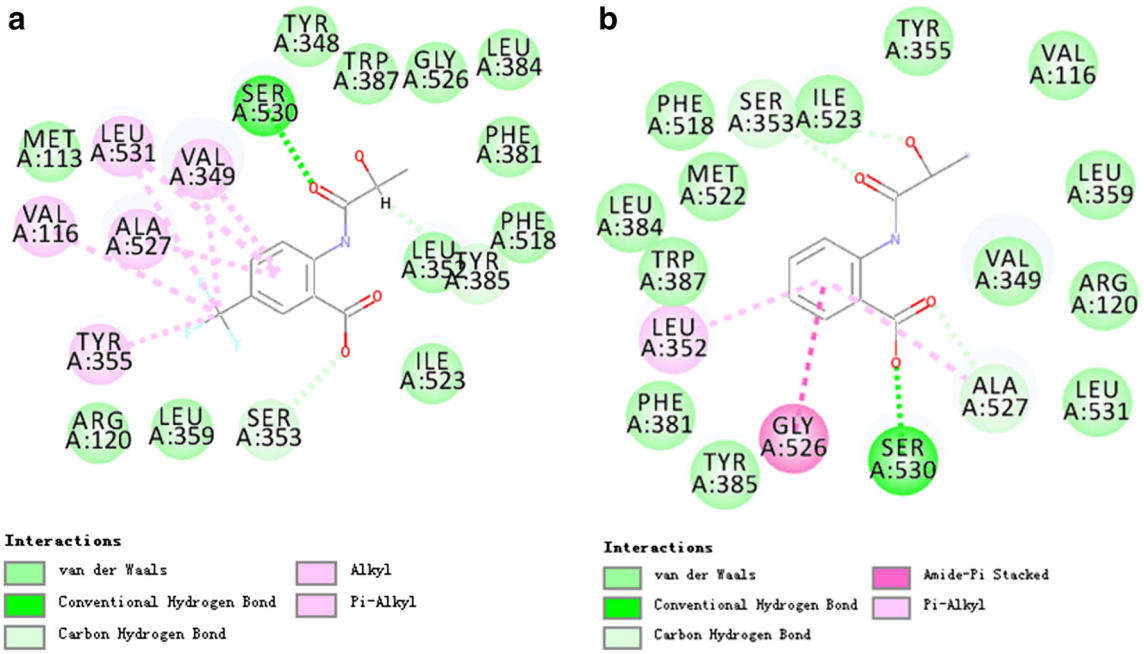

Fig. 5 Docked pose of compound **a** *R*-HFBA and **b** *R*-HPABA with COX-1

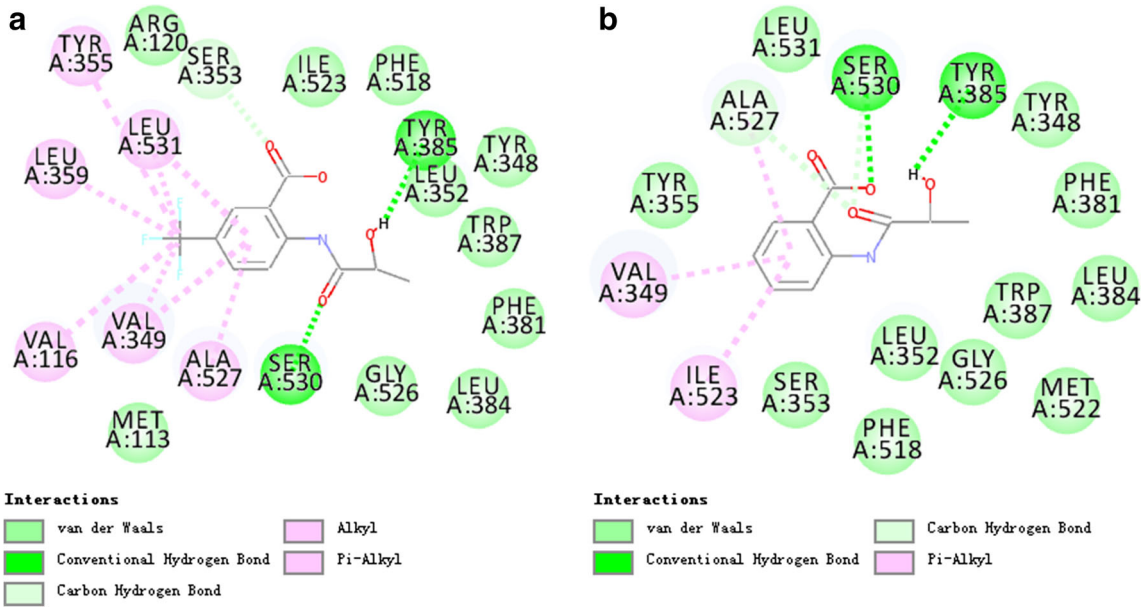

Fig. 6 Docked pose of compound **a** *S*-HFBA and **b** *S*-HPABA with COX-1

The quartet peaks at 4.28 ppm indicated the existence of linker (–CH–) group attach to amide group. Meanwhile, ^{13}C NMR spectra showed a singlet signal corresponding to –CONH– at 177.2 ppm and COOH group at 169.4 ppm, respectively. It also revealed the CF_3 group as quartet signals at 125.2 ppm.

The carrageenan-induced rat paw edema model comprises two phases. The first phase is mediated by releasing of pro-inflammatory mediators, such as histamine, serotonin, kinins, and occurs up to 2 h after the injection of carrageenan (Bhukya et al. 2009; Brooks and Day 1991). While the second phase (3–5 h after carrageenan injection) is relative to the release of prostaglandin, nitric oxide and cytokines, which is generated by an inducible COX-2 isoform. The second phase is sensitive to both steroidal and nonsteroidal anti-inflammatory agent used in clinical therapeutics (Matsumoto et al. 2015; Ishola et al. 2014). The edema produced in both early and late phase involves the release of mediators (e.g. prostaglandin, bradykinin), which later induces the biosynthesis of prostaglandin and other mediators. Inhibiting the synthesis of these mediators can effectively lead to the reduction of pain and inflammation

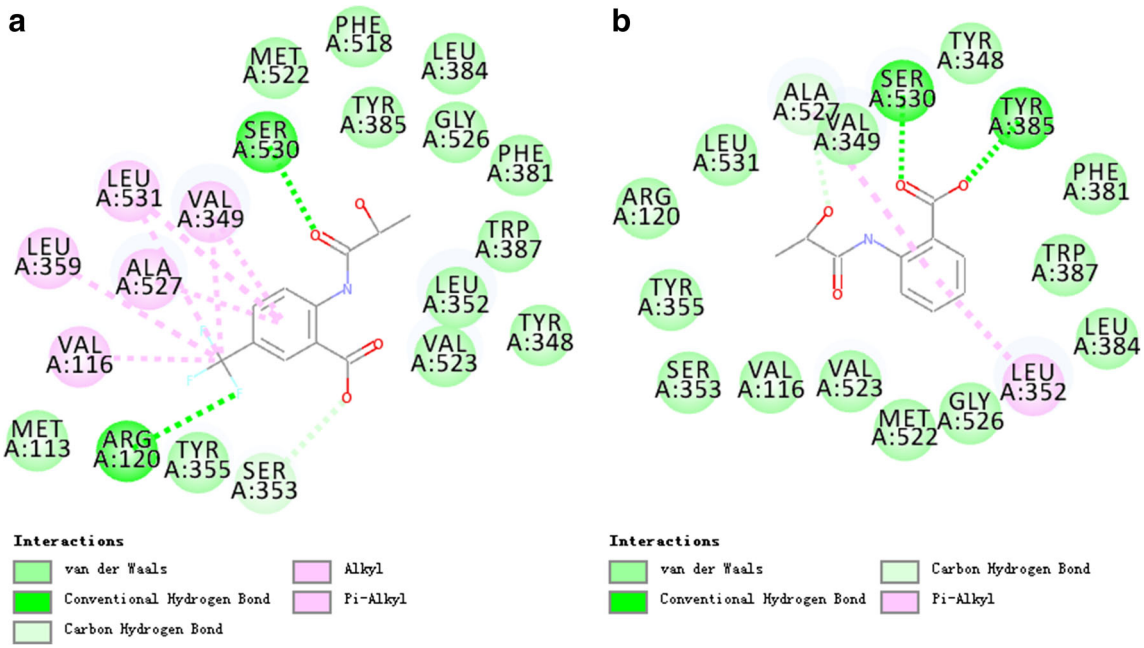

Fig. 7 Docked pose of compound **a** *R*-HFBA and **b** *R*-HPABA with COX-2

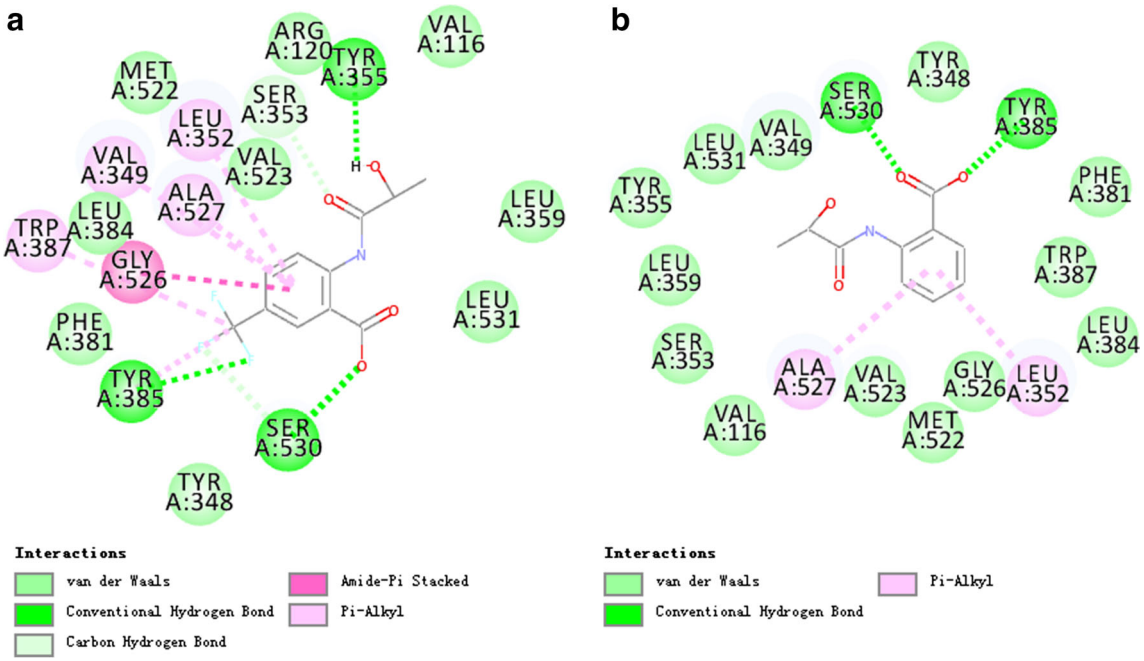

Fig. 8 Docked pose of compound **a** *S*-HFBA and **b** *S*-HPABA with COX-2

(Ueno et al. 2000). We found that *R*-/*S*-HFBA and *R*-/*S*-HPABA significantly inhibited rat paw edema in both phases, suggesting that the anti-inflammatory effect of these agents is involved with the inhibition of COX leading to the decrease of different inflammatory mediators. Our previous study also showed that the anti-inflammatory effect of HPABA was due to NO, malondialdehyde and PG suppression (data are not listed). In this study, *R*-/*S*-HFBA exhibited better results in inhibiting the second phase of carrageenan-induced paw edema than *R*-/*S*-HPABA, respectively. One explanation for this finding may be that *R*-/*S*-HFBA possess more potent COX inhibitory activity. Another one is likely due to the better pharmacokinetic properties of *R*-/*S*-HFBA.

As mentioned above, carrageenan injection can induce the release of proinflammatory cytokines. In order to investigate the effects of those compounds on the production of inflammatory cytokines, TNF-α and IL-1β levels in rat paws tissue were determined. TNF-α and IL-1β are the most important mediators of inflammatory responses since their over expression can provoke severe proinflammatory reactions. Our results showed that *R*-/*S*-HFBA could significantly attenuate the production of TNF-α and IL-1β in carrageenan-injected paws

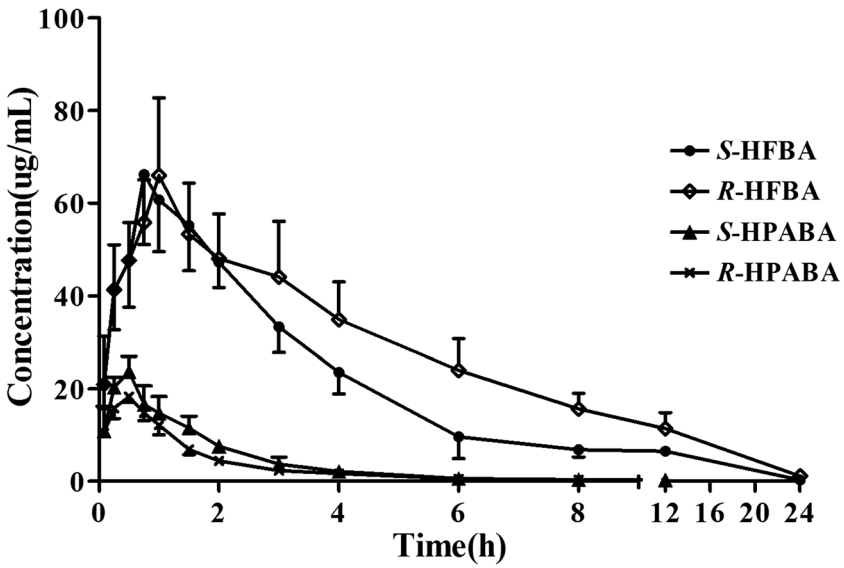

Fig. 9 Mean plasma concentration-time curves of *R*-/*S*-HFBA and *R*-/*S*-HPABA after intragastric administration of 50 mg/kg to rats ($n = 5$)

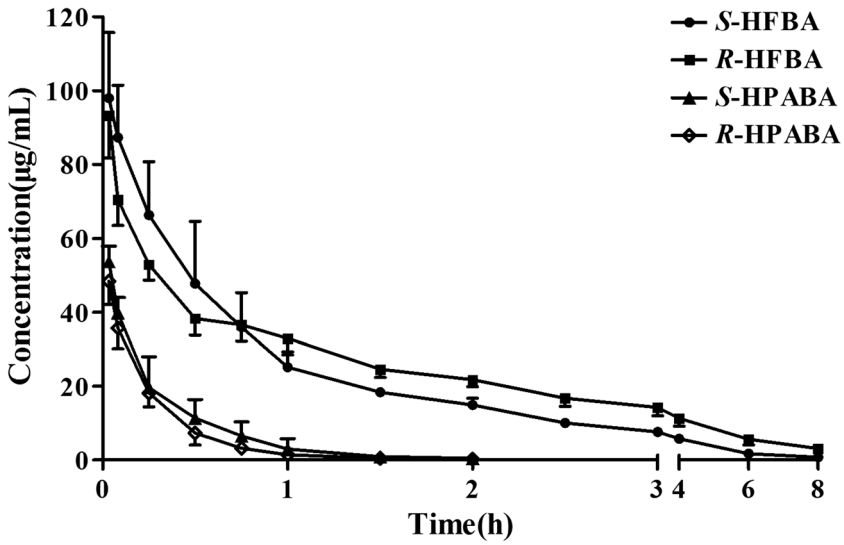

Fig. 10 Mean plasma concentration-time curves of *R*-/*S*-HFBA and *R*-/*S*-HPABA after intravenous administration of 12.5 mg/kg to rat ($n = 5$)

compared to *R*-/*S*-HPABA, respectively. These findings further demonstrated that *R*-/*S*-HFBA had better anti-inflammatory effect than *R*-/*S*-HPABA, respectively.

In platelets, AA is released by activation of phospholipase A_2 and metabolised by COX and lipoxygenases finally resulting in the generation of TXA_2 (Hubertus et al. 2014). TXA_2 is a potent stimulant of platelet aggregation leading to arterial thrombosis. Our previous study revealed that the anti-platelet aggregation effect of *R*-/*S*-HPABA was attributed to the inhibition of COX-1 enzyme resulting in a reduction of the proaggregatory product TxA_2 (Zhang et al. 2017). The results in this experiment showed that *R*-/*S*-HFBA had more effect on AA-induced platelet aggregation than *R*-/*S*-HPABA. So, the trifluoromethyl group found in *R*-/*S*-HFBA may contribute to their potent anti-platelet and inhibition of COX-1. Moreover, future studies on the antiplatelet aggregation effect of *R*-/*S*-HFBA in vivo are needed.

The purpose of the molecular docking is to evaluate the binding affinity of the compounds with observed pharmacological effect towards COX-1/COX-2 enzyme. It is worth mentioning that trifluoromethyl moiety imparted lipophilic properties to *R*-/*S*-HFBA which increased its affinity with COX-1/COX-2 active site by hydrophobic interactions. *R*-HFBA could have hydrophobic interactions with side chains of TYR355, VAL116, LEU531 and VAL349 through trifluoromethyl group in the COX-1 binding site. Likewise, the trifluoromethyl group of *S*-HFBA showed hydrophobic contact with TYR355, VAL116, LEU531, VAL349 and

Table 2 Main pharmacokinetic parameters of *R*-/*S*-HFBA and *R*-/*S*-HPABA after intragastric administration of *R*-/*S*-HFBA and *R*-/*S*-HPABA (50 mg kg^{-1}) to rats (mean ± SD, $n = 5$)

Parameters	*S*-HFBA	*S*-HPABA	*R*-HFBA	*R*-HPABA
C_{max} (μg mL^{-1})	66.55 ± 14.40**	23.74 ± 3.23	67.66 ± 15.56$^{\#\#}$	18.34 ± 1.28
$AUC_{0\text{-}t}$ (μg mL^{-1} h)	267.01 ± 51.68**	41.41 ± 3.41	413.93 ± 55.03$^{\#\#}$	31.54 ± 2.97
$AUC_{0\text{-}\infty}$ (μg mL^{-1} h)	271.90 ± 46.49**	41.99 ± 3.75	420.60 ± 56.07$^{\#\#}$	32.23 ± 2.73
$t_{1/2}$ (h)	2.83 ± 0.72*	1.73 ± 0.38	3.98 ± 0.47$^{\#\#}$	1.41 ± 0.27
CL (L h^{-1} kg^{-1})	0.19 ± 0.04**	1.20 ± 0.11	0.12 ± 0.02$^{\#\#}$	1.56 ± 0.13
T_{max} (h)	0.80 ± 0.11**	0.50 ± 0.00	0.90 ± 0.14$^{\#\#}$	0.50 ± 0.00

$^{*}p < 0.05$, $^{**}p < 0.01$ *S*-HFBA vs. *S*-HPABA, $^{\#}p < 0.05$, $^{\#\#}p < 0.01$ *R*-HFBA vs. *R*-HPABA

Table 3 Main pharmacokinetic parameters of *R*-/*S*-HFBA and *R*-/*S*-HPABA after intravenous administration of *R*-/*S*-HFBA and *R*-/*S*-HPABA (12.5 mg kg^{-1}) to rats (mean ± SD, $n = 5$)

Parameters	*S*-HPABA	*S*-HFBA	*R*-HPABA	*R*-HFBA
C_{max} (μg mL^{-1})	53.79 ± 4.20	98.01 ± 17.72	48.43 ± 6.26	116.62 ± 17.80
$AUC_{0\text{-}t}$ (μg mL^{-1} h)	17.81 ± 5.24	99.92 ± 13.16	14.01 ± 1.75	129.06 ± 11.56
$AUC_{0\text{-}\infty}$ (μg mL^{-1} h)	17.90 ± 5.34	101.77 ± 12.20	14.07 ± 1.76	139.22 ± 14.88
$t_{1/2}$ (h)	0.25 ± 0.03	1.55 ± 0.32	0.23 ± 0.05	2.27 ± 0.26
CL (L h^{-1} kg^{-1})	0.74 ± 0.19	0.12 ± 0.02	0.90 ± 0.10	0.09 ± 0.01

LEU359 in the COX-1. In addition to the hydrophobic interactions, *R*-HFBA also elicited hydrogen bonding interaction with side chains of ARG120 in COX-2 through fluorine atom. Also, trifluoromethyl moiety of *S*-HFBA showed H-bond interactions with TYR385 and SER530 which proved the importance of CF_3 as a pharmacophoric group in COX-2. In summary, the docking study results showed that *R*-/*S*-HFBA displayed better binding affinities to the target enzymes than *R*-/*S*-HPABA because of trifluoromethyl, respectively. Docking score also rationalised that the presence of trifluoromethyl group can lead to increase in activity. These results were in accordance with the anti-inflammatory antiplatelet aggregation activity assay described above, where inhibitory activity of *R*-/*S*-HFBA against COX-1/COX-2 was stronger than that of *R*-/*S*-HPABA.

The pharmacokinetic properties of *R*-/*S*-HFBA and *R*-/*S*-HPABA were investigated after intragastric and intravenous administration. When compared with *S*-HPABA, *S*-HFBA showed a longer $t_{1/2}$, a larger $AUC_{0\text{-}\infty}$ and a lower clearance rate after intragastric administration, which demonstrated that *S*-HFBA is more metabolically stable in vivo than *S*-HPABA. Similar results were also obtained in *R*-HFBA compared with *R*-HPABA, which demonstrated our hypothesis that trifluoromethyl group can block metabolism at the 5-position of the phenyl ring and that its electron withdrawing property generally invalidate the phenyl toward P450 enzyme-based aromatic hydroxylation. The excellent bioavailability of *R*-/*S*-HFBA is also consistent with their metabolic stability, resulting in more potent efficacy than *R*-/*S*-HPABA in vivo.

Conclusions

In summary, it was firstly confirmed that *R*-/*S*-HFBA represent more potent anti-inflammatory antiplatelet effect and better pharmacokinetic properties than *R*-/*S*-HPABA. Their docking experiments correlated with their biological activity and confirmed the high binding affinity towards COX-1/COX-2 due to the introduction of trifluoromethyl. Based on these researches, it could be convinced that *R*-/*S*-HFBA might be promising candidates for anti-inflammatory antiplatelet treatment. Of course, much more challenging studies still should be done in the future, such as metabolic mechanism, clinic pharmacokinetics and safety evaluation, etc.

Acknowledgments The authors thank School of Pharmaceutical Engineering, Shenyang Pharmaceutical University, Dr. Jian Wang, Dr. Youjun Xu for technical support in this study.

Authors' contributions RR, ZY and YZ conceived and designed this research. RR, ZR, WX and DY conducted experiments and analyzed the data. ZR was responsible for the synthesis of *R*-/*S*-HFBA. RR wrote the manuscript. All authors read and approved the manuscript.

Conflict of interest The authors declare that they have no conflict of interest.

References

Abid OR, Khalid M, Hussain MT, Hanif M, Qadeer G, Rama NH, Kornienko A, Khan KM (2012) Synthesis and anti-cancer, anti-metastatic evaluation of some new fluorinated isocoumarins and 3, 4-dihydroisocoumarins. J Fluor Chem 135:240–245

Acena JL, Sorochinsky AE, Moriwaki H, Sato T, Soloshonok VA (2013) Synthesis of Fluorine-Containing α-Amino Acids in Enantiomerically Pure Form via Homologation of Ni(II) Complexes of Glycine and Alanine Schiff Bases. J Fluor Chem 155:21–38

Ashour HM, Shaaban OG, Rizk OH, El-Ashmawy IM (2013) Synthesis and biological evaluation of thieno [2',3':4,5]pyrimido[1,2-b][1,2,4]triazines and thieno[2,3-d][1,2,4]triazolo[1,5-a]pyrimidines as anti-inflammatory and analgesic agents. Eur J Med Chem 62:341–351

Bhukya B, Anreddy RNR, William CM, Gottumukkala KM (2009) Analgesic and anti-inflammatory activities of leaf extract of Kydia calycina Roxb. Bangl J Pharmacol 4(2):101–104

Brooks PM, Day RO (1991) Nonsteroidal anti-inflammatory drugs–differences and similarities. N Engl J Med 324:1716–1725

Catella-Lawson F, Reilly MP, Kapoor SC, Cucchiara AJ, DeMarco S, Vyas SN, FitzGerald GA (2001) Tournier B, Cyclooxygenase inhibitors and the antiplatelet effects of aspirin. N Engl J Med 345(25): 1809–1817

Cho EJ, Senecal TD, Kinzel T, Zhang Y, Watson DA, Buchwald SL (2010) The Palladium-Catalyzed Trifluoromethylation of Aryl Chlorides. Sci 328:1679–1681

Dey R, Sultana S, Bishayi B (2018) Combination treatment of celecoxib and ciprofloxacin attenuate slive S. Aureus induced oxidative damage and inflammation in murine microglia via regulation of cytokine balance. J Neuroimmunol 316:23–29

Fiorucci S, Meli R, Bucci M, Cirino G (2001) Dual inhibitors of cyclooxygenase and 5-lipoxygenase. A new avenue in anti-inflammatory therapy. Biochem Pharmacol 62(11):1433–1438

Gillis EP, Eastman KJ, Hill MD, Donnelly DJ, Meanwell NA (2015) Applications of Fluorine in Medicinal Chemistry. J Med Chem 58: 8315–8359

Gouverneur V, Müller K (2012) Fluorine in Pharmaceutical and Medicinal Chemistry: From Biophysical Aspects to Clinical Applications. Imperial College Press, London

Guan J, Zhang QL, Rong R, Han F, Zhu HY, Zhao YL, Song AH, Yu ZG (2015) Metabolic profile of 2-(2-hydroxypropanamido) benzoic acid in rats by ultrahigh performance liquid Chromatography combined with Fourier transform ion cyclotron resonance mass Spectrometry. J Chromatogr B 993-994:60–68

Hagmann WK (2008) The Many Roles for Fluorine in Medicinal Chemistry. J Med Chem 51:4359–4369

Hasskarl J (2014) Sorafenib: targeting multiple tyrosine kinases in cancer. Recent Results Cancer Res 201:145–164

Helmersson J, Vessby B, Larsson A, Basu S (2005) Cyclooxygenase-mediated prostaglandin F2alpha is decreased in an elderly population treated with low-dose aspirin. Prostaglandins Leukot Essent Fat Acids 72(4):227–233

Hubertus K, Mischnik M, Timmer J, Herterich S, Mark R, Moulard M, Walter U, Geiger J (2014) Reciprocal regulation of human platelet function by endogenous prostanoids and through multiple prostanoid receptors. Eur J Pharmacol 740:15–27

Ishola IO, Agbaje EO, Adeyemi OO, Shukla R (2014) Analgesic and anti-inflammatory effects of the methanol root extracts of some selected Nigerian medicinal plants. Pharm Biol 52(9):1208–1216

Ismail FMD (2002) Important fluorinated drugs in experimental and clinical use. J Fluor Chem 118:27–33

Kulikova EA, Volcho KP, Salakhutdinov NF, Kulikov AV (2017) Benzopentathiepine Derivative, 8-(Trifluoromethyl)-1,2,3,4,5-Benzopentathiepin- 6-Amine Hydrochloride (TC-2153), as a Promising Antidepressant of New Generation. Lett Drug Des Discovery 14:974–984

Lazzaroni M, Bianchi PG (2004) Gastrointestinal side-effects of traditional non-steroidal anti-inflammatory drugs and new formulations. Aliment Pharmacol Ther 20:48–58

Liu X, Xu C, Wang M, Liu Q (2015) Trifluoromethyltrimethylsilane: Nucleophilic Trifluoromethylation and Beyond. Chem Rev 115: 683–730

Matsumoto K, Obara S, Kuroda Y, Kizu J (2015) Anti-inflammatory effects of linezolid on carrageenan-induced paw edema in rats. J Infect Chemother 21:889–891

Maurent K, Vanucci-Bacqué C, Baltas M, Nègre-Salvayre A, Augé N, Bedos-Belval F (2017) Synthesis and biological evaluation of diarylheptanoids as potential antioxidant and anti-inflammatory agents. Eur J Med Chem 144:289–299

Mueller K, Faeh C, Diederich F (2007) Fluorine in pharmaceuticals: looking beyond intuition. Sci 317:1881–1886

Newton K, Dixit VM (2012) Signaling in innate immunity and inflammation. Cold Spring Harb Perspect Biol 4(3):829–841

Ojima I (2013) Exploration of Fluorine Chemistry at the Multidisciplinary Interface of Chemistry and Biology. J Organomet Chem 78:6358–6383

Orlando BJ, Malkowski MG (2016) Substrate-selective Inhibition of Cyclooxygeanse-2 by Fenamic Acid Derivatives Is Dependent on Peroxide Tone. J Biol Chem 291(29):15069–15081 jbc.M116.725713

Palmer KJ, Holliday SM, Brogden RN (1993) Mefloquine. A review of its antimalarial activity, pharmacokinetic properties and therapeutic efficacy. Drugs 45:430–475

Purser S, Moore PR, Swallow S, Gouverneur V (2008) Fluorine in medicinal chemistry. Chem Soc Rev 37:320–330

Rao PPN, Kabir SN, Mohamed T (2010) Nonsteroidal Anti-inammatory Drugs (NSAIDs): progress in small molecule drug development. Pharm 3(5):1530–1549

Russo G, Paganotti GM, Soeria-Atmadja S, Haverkamp M, Ramogola-Masire D, Vullo V, Gustafsson LL (2016) Pharmacogenrtics of non-nucleoside reverse transcriptase inhibitors(NNRTls) in resourse-limited settings: influence on an -tiretroviral therapy responce and contominant anti-turbeculat, antimalarial and contraceptive treatments. Infect Genet Evol 37:192–207

Sayed MTE, Elsharief MAMS, Zarie ES (2018) Design, synthesis, anti-inflammatory antitumor activities, molecular modeling and molecular dynamics simulations of potential naprosyn® analogs as COX-1 and/or COX-2 inhibitors. Bioorg Chem 76:188–201

Sidhu RS, Lee JY, Yuan C, Smith WL (2010) Comparison of Cyclooxygenase-1 Crystal Structures: Cross-Talk between Monomers Comprising Cyclooxygenase-1 Homodimers. Biochem 49(33):7069–7079

Sorochinsky AE, Soloshonok VA (2010) Asymmetric Synthesis of Fluorine-Containing Amines, Amino Alcohols, α- and β-Amino Acids Mediated by Chiral Sulfinyl Group. J Fluor Chem 131:127–139

Tressaud A, Haufe G (2008) Fluorine and Health Malecular Imaging, Biomedical Materials and Pharmaceuticals. Elsevier Science Ltd.

Ueno A, Naraba H, Ikeda Y, Ushikubi F, Murata T, Naramiya S, Ohishi S (2000) Intrinsic prostacyclin contributes to exudation induced by bradykinin or carrageenin: a study on the paw edema induced in IP-receptor-deficient mice. Life Sci 66(12):155–160

Vane J, Botting R (1987) Inflammation and the mechanism of action of anti-inflammatory drugs. FASEBJ 1(2):89–96

Wang J, Sanchez-Rosello M, Acena JL, Pozo CD, Sorochinsky AE, Fustero S, Soloshonok VA, Liu H (2014) Fluorinein pharmaceutical industry: fluorine-containing drugs introduced to the Market in the last decade (2001-2011). Chem Rev 114:2432–2506

Wang JJ, Zhao YL, Men L, Zhang YX, Liu Z, Sun TM, Geng YD, Yu ZG (2014a) Secondary metabolites of the marine fungus Penicillium chrysogenum. Chem Nat Compd 50:405–407

Wang JJ, Zhao YL, An ZZ, Sun TM, Yu ZG (2014b) Synthesis and quantitative determination of the related substances of 2-(2-hydroxypropanamido) benzoic acid by RP-HPLC. J Shenyang Pharm Univ 31:21

Winter CA, Risely EA, Nuss GW (1962) Carrageenin-induced edema in hind paw of the rat as an assay for anti-iflammatory drugs. Proc Soc Exp Biol Med 111:544–547

Woo KJ, Kwon TK (2007) Sulforaphane suppresses lipopolysaccharide-induced cyclooxygenase-2 (COX-2) expression through the modulation of multiple targets in COX-2 gene promoter. Int Immunopharmacol 7(13):1776–1783

Yu ZG, Zhao YL, Wang JJ (n.d.). A kind of benzoic acid compounds and its preparation method and application, Z L 201210541957. 8

Zhang QL, Wang DL, Zhang MY, Zhao YL, Yu ZG (2017) Studies on New Activities of Enantiomers of 2-(2-Hydroxypropanamido) Benzoic Acid: Antiplatelet Aggregation and Antithrombosis. PLoS One 12(1):e0170334